Molecular Crystals and Liquid Crystals Incorporating Nonlinear Optics

Publication details, including instructions for authors and subscription information:
http://www.tandfonline.com/loi/gmcl17

Conduction Electron Spin Resonance in Organic Conductors: The Radical Cation Salt $(Fluoranthene)_2^+ PF_6^-$

G. Denninger [a]

[a] Universität Bayreuth and BIMF, D-8580, Bayreuth, F.R. Germany

Version of record first published: 06 Dec 2006.

To cite this article: G. Denninger (1989): Conduction Electron Spin Resonance in Organic Conductors: The Radical Cation Salt $(Fluoranthene)_2^+ PF_6^-$, Molecular Crystals and Liquid Crystals Incorporating Nonlinear Optics, 171:1, 315-331

To link to this article: http://dx.doi.org/10.1080/00268948908065804

Mol. Cryst. Liq. Cryst., 1989, Vol. 171, pp. 315–331
Reprints available directly from the publisher
Photocopying permitted by license only

Printed in the United States of America

Conduction Electron Spin Resonance in Organic Conductors: The Radical Cation Salt (Fluoranthene)$_2^+$ PF_6^-

G. DENNINGER

Universität Bayreuth and BIMF D-8580 Bayreuth, F.R. Germany

Radical cation salts of pure hydrocarbons are model systems for organic conductors. Electron spin resonance experiments in (Fluoranthene)$_2^+$ PF_6^- are reviewed with special emphasis on the elucidation of conduction band properties. Pulsed ESR measurements allow the direct determination of the diffusion constant of the electrons. Double resonance techniques like the Overhauser shift method allow a detailed investigation of the anisotropic hyperfine interaction of the conduction electrons with protons and ^{13}C. The Overhauser shift technique complements Knight shift experiments. The conduction band characteristics derived from these experiments are strongly influenced by the molecular orbitals.

1. CESR IN ORGANIC CONDUCTORS

In this contribution we will concentrate on the role of electron spin resonance (ESR) in studies of conduction electrons in organic conductors. Conduction electron spin resonance (CESR) is particularly suited to study the dynamics of the electronic transport mechanisms in organic conductors. The main reason is that, due to the low Z of the atoms in organic substances, the spin orbit coupling of the charge carriers is weak and the resulting CESR lines can be extremely narrow. This is in contrast to the situation in classical metals. The second reason is, that the hyperfine coupling of the electrons to magnetic nuclei gives rise to the phenomena of Knight shift, Overhauser shift, Dynamic Nuclear Polarization and nuclear spin lattice relaxation governed by the dynamics of the charge carriers. Unlike to most classical metals where isotropic interactions prevail due to the cubic symmetries, the interactions in organic conductors are highly anisotropic reflecting the molecular symmetry of the constituting molecules. Both ^1H and ^{13}C are accessible in pure hydrocarbons and can serve as "local probes" for the charge carriers.

Organic conductors can be roughly classified by their morphology: there is the group of polymers made conductive by "doping" and the group of charge transfer salts which can be made to crystallize in single crystals. Even if the polymers seem to be more promising regarding practical applications they seem to be very poor candidates to unravel the microscopic mechanisms of electronic conduction in organic materials. Single crystals of sufficient size and quality are a prerequisite for detailed investigations. We have concentrated our research efforts mainly on the

study of radical cation salts of small aromatic hydrocarbons with inorganic counterions like PF_6^-, AsF_6^-, SbF_6^-. The organic constituent of these salts are from the group of aromatic ring systems like naphtalene, perylene, pyren or fluoranthene. These radical cation salts can serve as model systems for organic conductors as will be explained in the next chapter.

2. RADICAL CATION SALTS AS MODEL SYSTEMS FOR ORGANIC CONDUCTORS

An organic conductor is a substance where the conductivity is derived from electrons which are responsible for the binding of the organic molecules, i.e. the conductivity arises from molecular orbitals derived from s- or p-type atomic orbitals. It turns

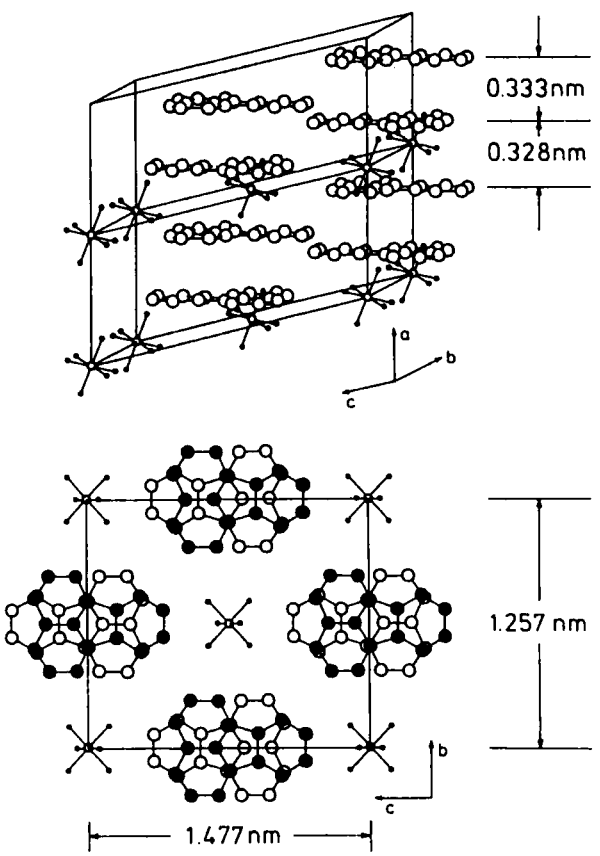

FIGURE 1 Crystal structure of $(FA)_2^+PF_6^-$ as determined by Enkelmann.[5] *Upper part:* Unit cell. The distances are for 300 K. The fluoranthene molecules are dimerized along the stacking axis *a*. *Lower part:* Projection onto the *b*,*c* plane. The PF_6^- counterions occupy the positions in the empty "channels" between the (FA) molecules.

out that the conduction phenomena are mainly attributable to the π-electron systems of either conjugated polymer chains or aromatic ring systems. In the first case it is the overlap between adjacent π-orbitals coupling along the chain that give rise to the conduction band. In the second class it is the overlap perpendicular to the plane of the aromatic ring systems which is important for forming the conduction band. In both cases it is essential that the band formed is partially empty to enable electrical conduction. This is accomplished by a partial or total charge transfer from the organic molecule to a counterion. Oxidation of the organic molecules leads to *p*-type conduction, whereas reduction would yield *n*-type conduction. If both constituents (donor and acceptor molecule) are organic, the charge transfer is often incomplete. The radical cation salts with inorganic counterions show distinct advantages for studying the conduction phenomena:

a) The charge transfer between the organic molecules and the inorganic ion is complete due to the large electronegativity difference.

b) The conduction phenomenon is nearly completely governed by the aromatic constituents, since the counterions form closed-shell subsystems.

c) Many radical cation salts show perfect stoichiometry and crystallize in single crystals.

The main disadvantage is, that they represent only one class of organic conductors and are only restricted models for conducting polymers like for example doped polyacetylene. Since the first report on the electrochemical crystallization of the radical cation salt of naphthalene and fluoranthene (FA) with suitable counteranions[1-3] these salts have aroused considerable interest. This interest multiplied when a narrow spin resonance line was detected and could be attributed to the conduction electrons.[4] Figure 1 shows the crystal structure of $(FA)_2^+ PF_6^-$.[5] The (FA) molecules are arranged in stacks and the counterions occupy channels in between. The crystals show a stoichiometry of 2:1, which means that within the (FA) stack 1 electron is lacking per dimer as compared to the neutral stack. The molecules are slightly dimerized along the stacking direction as shown by the distances 0.333 nm and 0.328 nm. Therefore, the conduction band is half filled.

The ESR originates from the charge carriers. This has been demonstrated by a series of experiments some of which are presented below. The crystals are conducting along the stacking axis *a* with conductivities between 100–1000 $(\Omega cm)^{-1}$ at 300 K.[6] The value of the conductivity perpendicular to the stacking direction is smaller by at least a factor of 1000. These quasi "one-dimensional" properties of the charge carriers are reflected in the spin dynamics of the electrons and the magnetic nuclei. At $T \simeq 180$ K a phase transition to a semiconducting state occurs. We will concentrate on the high temperature "metallic" phase only.

3. CW—CONDUCTION ELECTRON SPIN RESONANCE

A strong ESR signal is observed in the temperature range between 300 K and 180 K. This regime is called "metallic." There are numerous investigations supporting

the notion of electrons forming a Fermi system and being responsible for the observed conduction phenomenon:

i) The static magnetic susceptibility is dominated by the contribution from the electrons above 180 K.[7]

ii) The proton spin lattice relaxation rate is proportional to the temperature T between 180 K and 300 K.[8,9] This Korringa-type behaviour is a strong indication for mobile electrons obeying Fermi–Dirac statistics.

iii) Optical reflection measurements[10] and thermopower investigations[11] on similar radical cation salts indicate a "metallic" conduction band with a tight-binding bandwidth of $4t_{\parallel} = 2.25$ eV.

iv) The temperature dependence of the observed ESR-signal is identical to the measured static susceptibility above 180 K. The absolute intensity of the ESR-signal shows that every $(FA)_2$ dimer contributes one electron to a one-dimensional band with a Fermi-temperature of $T_F \simeq 2200$ K.[9]

The observed resonance signal has a Lorentzian line shape in the region 300 K to 180 K. The linewidth depends somewhat on crystal quality: it varies between 1 μT–2 μT at 300 K and has a minimum of 0.8 μT at 200 K. In frequency units this corresponds to 22 kHz. This is a remarkably small value for the solid state. This value already shows that the electrons must be either mobile or that rapid spin diffusion can take place. Both would lead to motional narrowing of the interactions that are present in the solid state. If one considers only the hyperfine interaction with the 20 protons on one dimer, the observed linewidth would be roughly 14.5 MHz. The observed linewidth is 3 orders of magnitude smaller. One has to conclude that the correlation time τ_c of the spin at one dimer position is considerably smaller than the Larmor precession period of 10^{-10} sec. If one considers the dipolar coupling between two spins on adjacent dimers, this would lead to a linewidth of ≃200 MHz. Taking the Anderson-Weiß formula[12] connecting the observed linewidth $\Delta f_{obs} = (\langle \Delta f_{dip} \rangle^2) \cdot \tau_c$ with the expected linewidth Δf_{dip} due to the dipolar coupling, we can calculate an upper limit of the correlation time $\tau_c < 8 \cdot 10^{-13}$ s. Analyzing the diffusion constant of the electrons yields an actual value of $\tau_c = 3 \cdot 10^{-15}$ s. This value of the correlation time and the low efficiency of spin-orbit coupling as a source of relaxation for the electrons is the clue to the exceptionally narrow linewidths observed for the whole class of radical-cation salts built from pure hydrocarbons. The role of spin-orbit coupling is analyzed in connection with the observed *g*-factors.

The skin depth of our samples at 10 GHz is ≃30 μm for σ (300 K) = 300 $(\Omega cm)^{-1}$. Considering the typical sample dimensions (1000 μm × 100 μm × 100 μm) one would expect non-Lorentzian line shapes according to the theory of Dyson.[13] This is not observed experimentally. The reason is that in highly anisotropic conductors the influence of the skin depth is reduced considerably. Qualitatively one should consider the conductivity $\sigma_{\perp}$ instead of $\sigma_{\parallel}$, yielding a modified skin depth of ≃3 mm. A more detailed analysis[14] shows, that only small deviations from a Lorentzian signal are expected in our case.

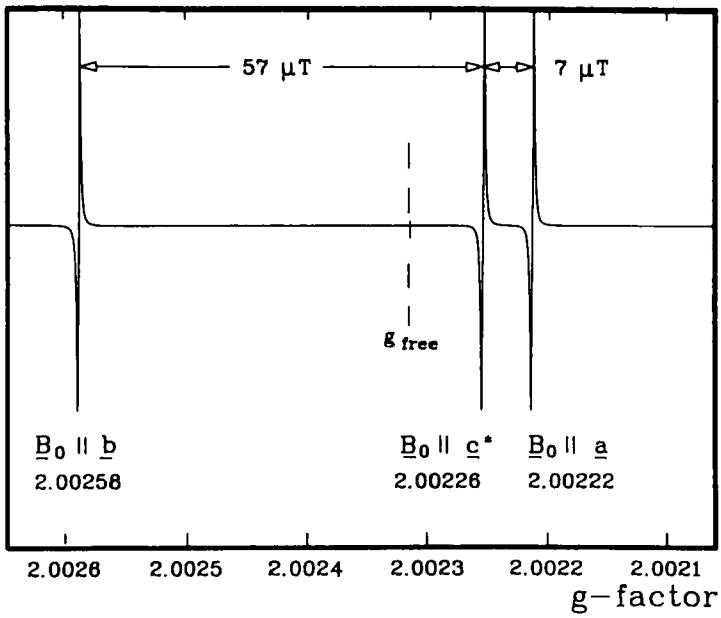

FIGURE 2 The g-factor of $(FA)_2^+PF_6^-$ along the three principal axes: g_{aa} = 2.00222(2); g_{bb} = 2.00258(2); $g_{c^*c^*}$ = 2.00226(2). a is parallel to the needle axis of the crystals.

4. THE g-FACTOR AND ITS ANISOTROPY

Figure 2 shows the g-factor of $(FA)_2PF_6$ along the three principal axes. We have measured the g-factor with the "internal" ^1H standard via the Overhauser shift (Chapter 7). The *absolute* accuracy is better than $1 \cdot 10^{-5}$. The value g_{zz} = 2.00222(2) is parallel to the stacking axis a. An analysis of a crystal where the b and c axes are indicated by the crystal morphology shows that g_{xx} = 2.00258(2) is along the b axis and g_{yy} = 2.00226(2) is along c^*. The deviations from g_{free} are:

$$a: \quad \Delta g_{aa} = -(9.9 \pm 1) \cdot 10^{-5}$$

$$b: \quad \Delta g_{bb} = +(26.1 \pm 1) \cdot 10^{-5}$$

$$c^*: \quad \Delta g_{c^*c^*} = -(5.9 \pm 1) \cdot 10^{-5}$$

The mean deviation is $\langle \Delta g \rangle = 1/3 \cdot (\Delta g_{aa} + \Delta g_{bb} + \Delta g_{c^*c^*}) = (3.4 \pm 1) \cdot 10^{-5}$. The largest deviations from g_{free} occur along b, whereas $\Delta g_{c^*c^*}$ is small. One can compare the values to a theory of g-factors for aromatic radical cations[15,16] and to measurements[16,17] in solutions. The theory predicts a positive shift along the b axis for $(FA)^+$ and no shift along the mirror axis c^*. The negative value along the a

axis is a general property of aromatic molecules and can be understood quantitatively by a more elaborate theory including relativistic effects.[18]

We conclude that the measured g-tensor is consistent with the model of a conduction electron band derived from the π-orbital of the $(FA)_2$ dimers. It is interesting to use the measured deviation $\langle \Delta g \rangle$ for a calculation of the expected T_1 and T_2 times of the ESR due to the Elliot mechanism.[19,20] This mechanism connects the spin-flip rate $1/T_2$ of the electrons with the phonon-induced scattering time τ_c which determines e.g. the electrical conductivity. The spin-flips are induced by the small residual spin-orbit interaction. In the 3-dimensional isotropic case the Elliot-mechanism predicts:

$$1/T_2 = (\Delta g)^2/\tau_c$$

where Δg is taken to be proportional to the spin-orbit interaction. Taking $\tau_c = \tau_\parallel = 3 \cdot 10^{-15}$ s (Ch. 5) and $\Delta g = \Delta g_{bb} = 26 \cdot 10^{-5}$ we get $1/T_2 = 2.25 \cdot 10^7\ s^{-1}$ and $T_2 = 44$ ns. The measured value of $T_2 \simeq 10$ μs shows, that the Elliot mechanism cannot be applied to the one-dimensional case without modifications. One suggested solution is to use the scattering time $\tau_\perp$ instead,[21] which would lead to a considerably longer $T_2 \cdot A\ \tau_\perp = 3 \cdot 10^{-12}$ sec would yield $T_2 = 44$ μs. The Elliot mechanism could contribute part of the linewidth in the radical cation salts.

5. DETERMINATION OF THE DIFFUSION CONSTANT OF THE ELECTRONS BY ESR

A Lorentzian line with $\Delta f_{pp} = 20$ kHz corresponds to a free induction signal of the form $M_x(t) = M_o \cdot \exp(-t/T_2)$ with $T_2 = 9.19$ μs. $M_x(t)$ is the transverse magnetization in the rotating frame. This exceptionally long value of T_2 opened the way for pulsed ESR-measurement using modified CW-spectrometers or even NMR-spectrometers for ESR at 190 MHz.[6,22,23] The T_1 and T_2 times as a function of temperature were determined that way.[24] Diffusion of the spins in a constant gradient G lead to a faster decay of the echo amplitude $A(\tau)$ in a Hahn spin-echo experiment[25]:

$$A(\tau) = A_o \cdot \exp(-2 \cdot \tau/T_2) \cdot \exp(-2/3 \cdot \gamma^2 \cdot G^2 \cdot D \cdot \tau^3) \qquad (1)$$

$A(\tau)$ is the spin-echo amplitude, γ the magnetogyric ratio of the diffusing spins and D is the diffusion constant. In an anisotropic solid the diffusion "constant" is again a tensor and by suitable orientation of the single crystal sample with respect to B_o the three components D_{xx}, D_{yy}, and D_{zz} have been determined.[44]

Figure 3 shows $\log(A(\tau))$ versus τ for two orientations of the crystal axes with respect to B_o.[24] For $a \perp B_o$ an analysis according to (1) yields an upper limit $D_\perp \leq 1.2 \cdot 10^{-3}$ cm²/s. For the $a \parallel B_o$ case the additional quadratic term $-1/3 \cdot \gamma^2 \cdot G^2 \cdot D \cdot \tau^2$ is directly visible and leads to $D_\parallel = (1.3 \pm 0.3)$ cm²/s. These measurements have been extended and improved considerably by the group of Mehr-

ing.[26,27] By using a pulsed gradient G, they lowered significantly the limit for the determination of the diffusion term $D_\perp$. Both values $D_\parallel$ and $D_\perp$ are only slightly dependent on temperature, but they depend somewhat on sample quality. For $(FA)_2PF_6$ typical values are:

$$D_\parallel = (1.3 \pm 0.3)\ \text{cm}^2/\text{s} \quad \text{and} \quad D_\perp < 1 \cdot 10^{-3}\ \text{cm}^2/\text{s}$$

What is the connection between D and the conduction mechanism? A determination of $D \neq 0$ only signifies that the magnetization M diffuses. This diffusion can be caused by an actual motion of the electrons or by spin-diffusion. Assuming an electron band with a Fermi energy $E_F = 0.19$ eV we can calculate the following relations:

$$\tau_\parallel = D_\parallel/(v_F)^2 = 1.9 \cdot 10^{-15}\ \text{s} \tag{2a}$$

$$\mu_\parallel = e/m \cdot \tau_\parallel = 3.34\ \text{cm}^2/\text{Vs} \tag{2b}$$

$$\sigma_\parallel = n \cdot e \cdot \mu_\parallel = 435\ (\Omega\text{cm})^{-1} \tag{2c}$$

$$\lambda = v_F \cdot \tau_\parallel = 0.5\ \text{nm} \tag{2d}$$

v_F is the Fermi-velocity, $\tau_\parallel$ is the scattering time parallel to the stacking axis a, $\mu_\parallel$ is the mobility of the diffusing spins, $\sigma_\parallel$ is the corresponding conductivity and λ is

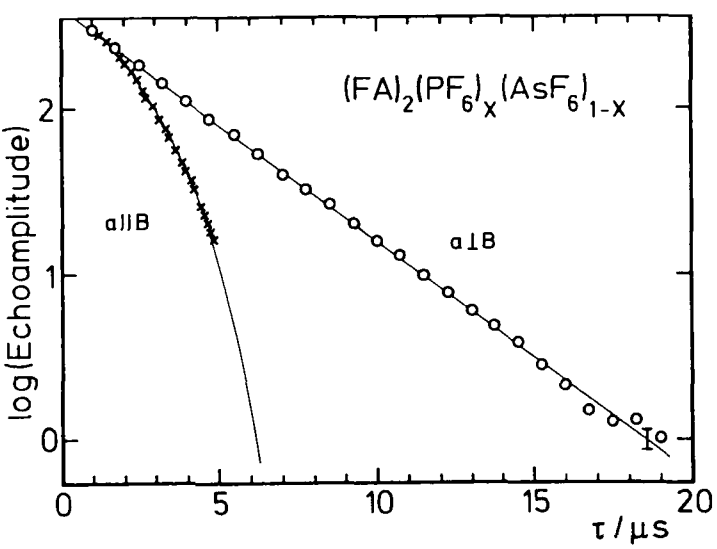

FIGURE 3 Logarithm of the spin-echo amplitude $A(\tau)$ versus τ in a constant gradient G. For $a \perp B_o$, an essentially monoexponential decay is observed. For $a \parallel B_o$, the diffusion constant $D_\parallel$ is indicated by the additional decay proportional to $-\tau^2$.

the mean free path. These values are in rather good agreement with the dc-conductivity. However, the rather short mean free path λ of only $\simeq$1 dimer distance shows, that the application of a free electron gas model is not allowed. Furthermore, there is experimental evidence that the magnetic field gradient method measures a "macroscopic" $D_{\parallel}$ influenced by paramagnetic impurities present in the crystals.[28] The "true" microscopic diffusion constant $D_{\parallel}$ could be one order of magnitude larger. However, there is still no direct measurement of this quantity.

We conclude, that the diffusion of the electronic spin can be directly measured with ESR methods. One can correlate these measurements with models of the conductivity and get good agreement consistent with electronic motion.

6. HYPERFINE INTERACTION OF THE CONDUCTION ELECTRONS

The coupling of the conduction electrons to nuclei with a magnetic moment μ_n is the source for a variety of effects. Due to the short correlation time τ_c of a conduction electron at a given nucleus, the hyperfine interaction is characterized by a few typical effects found usually in metals:

1) The polarization of the electron system in an applied field B_o leads to a shift of the NMR, the Knight shift.

2) The nuclear spin-lattice relaxation time T_1 is nearly completely dominated by the relaxation via the electron system. The T_1 times are much shorter than in similar solids without conduction electrons. The temperature dependence $T_1 \cdot T = \text{const}$ (Korringa law)[29] is typical for this situation and is a strong indication for the presence of conduction electrons.

3) The average polarization of the nuclei leads to a shift of the ESR resonance, the Overhauser shift.[30] This shift is usually very small and hard to measure, but it is large in the case of our organic conductors. This is due to the "Overhauser-effect," which leads to

4) the "Dynamic Nuclear Polarization" (DNP). By saturating the ESR of the conduction electrons, the nuclear polarization of hyperfine coupled nuclei can be significantly enhanced. This in turn enhances the Overhauser shift and can be used as a sensitive method to investigate the hyperfine interaction.

In pure hydrocarbons the protons are obvious candidates for studies of the hyperfine interactions. Due to the low natural abundance of only 1.1%, ^{13}C is difficult to measure, but sensitive techniques have been developed. The counterions like PF_6^- are accessible as well. Deuteration of the aromatic constituent and selective enrichment with ^{13}C at specific positions can vastly increase the knowledge gained from these hyperfine interaction experiments. Experiments directed towards the elucidation of the spin-density distribution in these radical cation salts will be presented in the next chapter.

The common source of all these phenomena is the interaction between an electron magnetic moment $\mu_e = \hbar \cdot \gamma_e \cdot S$ and a nuclear magnetic moment $\mu_n = \hbar \cdot \gamma_n \cdot I$ usually written in the operator form

$$H_{en} = I \cdot A \cdot S \tag{3}$$

with the hyperfine tensor A describing the interaction. Two contributions to the tensor A are usually distinguished: The dipolar interaction energy E between the two magnetic moments a distance r apart:

$$E_{dip} = (\mu_o/4\pi) \cdot (\mu_e \cdot \mu_n/r^3 - 3 \cdot (\mu_e \cdot r) \cdot (\mu_n \cdot r)/r^5) \quad (4)$$

and the Fermi-contact interaction

$$H_{fc} = -(8\pi)/3 \cdot (\mu_o/4\pi) \cdot \mu_e \cdot \mu_n \cdot |\Psi(0)|^2 \quad (5)$$

where $|\Psi(0)|^2$ is the conduction electron density at the nucleus. The contact interaction requires the wavefunction of the electron to be non-vanishing at the nuclear position. This is the case for s-type wave-functions. For a pure p- or d-type wavefunctions the contact interaction vanishes due to symmetry. However, in most organic radicals a scalar "pseudocontact" interaction with considerable size is observed. This is due to the core-polarization effect. In general, one expects the total interaction in hydrocarbons to be anisotropic due to the dipolar term (4). It turns out, that the electron-^{13}C interaction is very anisotropic and even for the proton hyperfine-interaction the anisotropy cannot be neglected.

Most pronounced are anisotropic Knight shifts and Overhauser shifts, but even spin-lattice relaxation rates depend on angle and position. Relations like the Korringa relation rely on an isotropic hyperfine interaction and can no longer be applied without caution in organic conductors. This will be made clear in the next chapter.

7. OVERHAUSER SHIFT AND KNIGHT SHIFT

For a radical in solution, the hyperfine interaction (hfi) $H_{en} = I \cdot A \cdot S$ usually leads to a resolved hyperfine structure of the ESR spectrum. If the electron is coupled to many nuclei or if the hyperfine couplings are small compared to the ESR-linewidth, an unresolved hyperfine structure leads to ESR line-broadening. The coupling can be investigated by ENDOR.[31] If however the correlation time τ_c of the electron at a nuclear position gets much smaller than the time scale of the hfi, the ESR spectrum coalesces into a single line. Thus, for $\tau_c \ll h/|A|$, where $|A|$ is the trace of A, the hfi seems to be completely eliminated. This is the situation in metals and in the radical cation salts as well.

Due to the nonzero polarizations P_n and P_e of the nuclei and the electrons in the static field B_o a residue of the hfi remains: the longitudinal component "shifts" the resonance. For a nuclear spin I = 1/2 and S = 1/2 this shift is given by:

$$\Delta f_n = 1/2 \cdot (A_{zz}/h) \cdot P_e \quad (6)$$

$$\Delta f_e = 1/2 \cdot (A_{zz}/h) \cdot P_n \quad (7)$$

Δf_n and Δf_e are the shifts of the NMR resp. the ESR, A_{zz} is the component of the hyperfine tensor in the B_o direction and P_e, P_n are the polarizations.

Equation (6) is the well known Knight shift written in an unfamiliar, but instructive, way. The complementary relation (7) is the Overhauser shift. At room temperature $P_e >> P_n$ for most metals, and the Knight shift exceeds the Overhauser shift. At low temperatures however, the Overhauser shift becomes quite sizable in metals like Li and in semiconductors. Most experiments were done at 4 K,[32] and only one application to organic conductors was reported.[33] For a metal with a density of states D(E) the polarization P_e is

$$P_e = 1/2\ (\hbar \cdot \gamma_e \cdot B_o) \cdot D(E_F) \tag{8}$$

where $D(E_F)$ is the density of states at the Fermi energy and $\hbar \cdot \gamma_e$ is the electron magnetic moment. With the NMR frequency $f_n = \hbar \cdot \gamma_n \cdot B_o$ we can reformulate (6) to

$$K := \Delta f_n/f_n = 1/4 \cdot (\gamma_e/\gamma_n) \cdot A_{zz} \cdot D(E_F) \tag{9}$$

K is the usual definition of the Knight shift. Equation (9) is only valid, if $T_F >> T$.

Due to the Curie behavior of the nuclear spins, P_n is given by

$$P_n = \tanh(\hbar \cdot \gamma_n \cdot B_o/(2\ kT)) \simeq \hbar \cdot \gamma_n \cdot B_o/(2\ kT) \tag{10}$$

With $f_e = \hbar \cdot \gamma_e \cdot B_o$, we define the Overhauser shift:

$$D := \Delta f_e/f_e = 1/4 \cdot (\gamma_n/\gamma_e) \cdot A_{zz}/kT \tag{11}$$

Comparing Knight shift and Overhauser shift, the ratio

$$K/D = (\gamma_e/\gamma_n)^2 \cdot k \cdot T \cdot D(E_F) \tag{12}$$

is independent of the A_{zz} and can be used to measure directly the density of states at the Fermi energy. Thus a combined determination of the Knight shift and the Overhauser shift yields direct information on the conduction electron band without additional assumptions. This analysis is now possible for the organic conductor $(FA)_2^+PF_6^-$, where the ^1H and ^{13}C Knight shifts have been determined by the group of Mehring[34–36] and the Overhauser shift in our work.[9,37,38] In addition, we have undertaken a simultaneous determination of both shifts for ^1H which will be presented elsewhere.[39]

By sweeping a saturating radiofrequency field ν_{rf} through the nuclear resonance position, one observes a shift of the ESR. This shift versus radiofrequency is shown in Figure 4 for the protons in $(FA)_2PF_6$. By a suitable choice of the radiofrequency power, a "spectrum" analogous to the NMR is obtained. However, it is not a spectrum of intensity versus frequency but rather interaction versus frequency. The width of 22 kHz FWHM is typical for a proton solid state spectrum and is explained quantitatively by the proton–proton dipolar interaction. More important is the

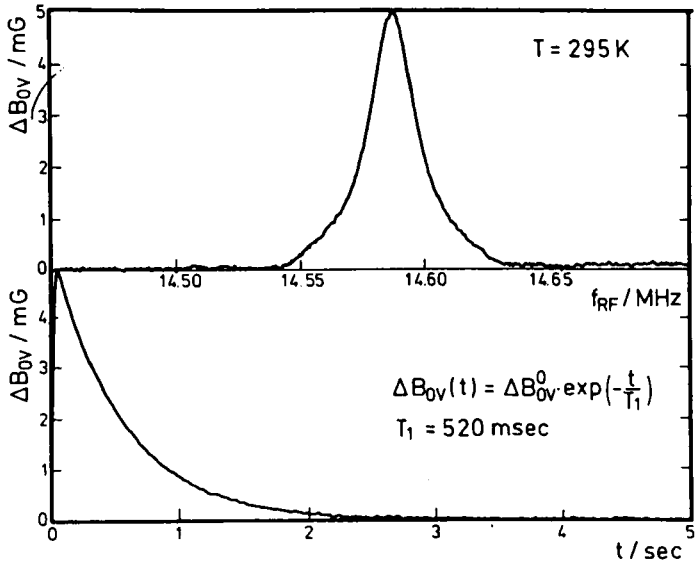

FIGURE 4 Overhauser shift of the protons in $(FA)_2^+ PF_6^-$ at room temperature. Larmor frequency ≃ 14.55 MHz. *Upper part:* Shift versus radiofrequency. The shift amounts to approx. half the ESR linewidth. *Lower part:* Shift versus time after switching off the saturating NMR frequency. A mono-exponential decay with T_1 = 520 msec is observed.

maximum shift value at resonance. With B_o = 0.34 T we calculate $D = -\Delta B_{ov}/B_o = -1.47 \cdot 10^{-6}$. This is very large!

The expected hfi for protons in aromatic hydrocarbons is known and is $A_{zz} = a \cdot h$ with $a = -65$ MHz. This is the isotropic hfi for a π-orbital radical. Thus we predict an Overhauser shift $D_o = -4.02 \cdot 10^{-9}$ at 295 K. The observed shift (Figure 4) is enhanced by a factor of 366. This enhancement of D is caused by the Dynamic Nuclear Polarization (DNP) or Overhauser effect. By partially saturating the ESR, the nuclear spin polarization is enhanced by a factor $D = D_o \cdot (1 + V \cdot S)$, where S is the saturation parameter of the ESR ($0 \leq S \leq 1$). For pure scalar coupling (contact interaction) $V = \gamma_e/\gamma_n = 658$ for protons. For pure dipolar coupling we would have $V = -1/2 \cdot \gamma_e/\gamma_n = -329$. Details are found in the paper by Solomon.[40] Measurement of V by classical NMR methods for the system $(Perylene)_2X^-$ have been reported.[41] We have analyzed in detail the dependence of V on temperature and orientation.[9] The main result is that V depends strongly on orientation and only slightly on temperature. For $B_o \parallel a$, $V_\parallel = 275 \pm 20$ and for $B_o \perp a$, $V_\perp = 525 \pm 40$. We see that the coupling is predominantly scalar, but that significant dipolar contributions enter for $B_o \parallel a$. A detailed analysis is found in Reference 9.

With both D and V determined in our experiment, we deduce an average hyperfine coupling of $\langle A_{zz}\rangle/h = (65 \pm 2.8)$ MHz. This value immediately signifies that,

1) The conduction electrons are derived from the π-orbital of the fluoranthene molecule, and

2) The conduction electrons are restricted nearly completely to the aromatic stack.

From Equation (12) with $D_o = -4 \cdot 10^{-9}$ (295 K) and the sum of the proton Knight shifts from Reference 35 ($K = -128 \cdot 10^{-6}$) we evaluate the density of states $D(E_F) = 2.93\ (eV)^{-1}$.

A one-dimensional free electron model with $m = m_o$ yields $D(E_F) = 2.24\ (eV)^{-1}$ (half filled band).

An important parameter of the conduction electron band can thus be determined by magnetic resonance techniques alone. One disadvantage of the proton measurements has to be mentioned at this point. Due to the large dipolar coupling, the individual proton positions cannot be resolved by the Overhauser shift technique. Only the average Overhauser shift can be determined. This is not sufficient to determine the spin-density distribution of the conduction electrons on the molecule. ^{13}C seems to be a more promising candidate to achieve resolution to individual positions. Due to the low natural abundance of 1.1%, the Overhauser shift signals are small and the measuring technique had to be improved to measure D shifts in the ppb (10^{-9}) range. Figure 5 shows the result for two different orientations of the crystal. With $B_o \parallel a$ the measured signal is rather large (-125 ppb). Since our measurement signal is $-D$ (we switch off the nuclear polarization), this corresponds to $D_a = 125 \cdot 10^{-9}$. For $B_o \parallel c^*$, $D_{c^*} = -15$ ppb. The value along b, not shown in Figure 5, is essentially equal to D_{c^*}. Unlike the proton case, ^{13}C shifts are highly

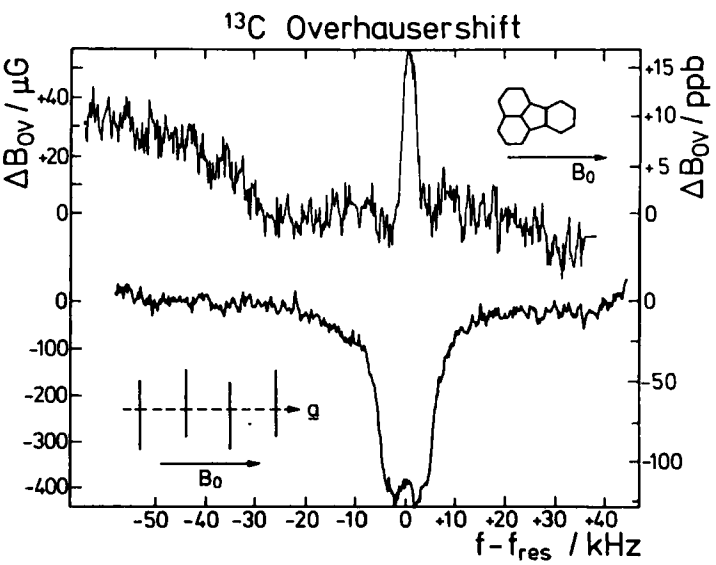

FIGURE 5 Overhausershift of ^{13}C in $(FA)_2^+ PF_6^-$ for two orientations of the field B_o. *Upper part:* with $B_o \parallel c^*$, a small positive shift of $\simeq$15 ppb is observed. *Lower part:* with $B_o \parallel a$ the shift amounts to $\simeq -125$ ppb with a characteristic splitting of the resonance due to nearest neighbor ^{13}C–^1H interaction.

anisotropic, even reversing sign in different orientations. Without an exact quantitative treatment, the following information can be gained:

1) Considering the natural abundance and the γ_n of ^{13}C the $D_a = 125$ ppb would correspond to 11.4 ppm for protons. The coupling of ^{13}C to the electrons is stronger than the coupling to the protons.

2) Since $D_a \simeq -8 \cdot D_{c*} \simeq -8 \cdot D_b$, we conclude that the tensor components of the ^{13}C hyperfine tensor at the individual positions must be axially symmetric and that the components in the direction perpendicular to the aromatic plane must be a factor of ≈8 larger than the components in the plane. This and the changing sign is consistent with the conduction electron occupying a π-orbital derived from carbon-p_z type orbitals.

The apparent T_1 for the shifts in the different directions is very different as well (Figure 6). Whereas the 125 ppb component builds up with $T_1 \simeq 5$ sec, the small −15 ppb component has a $T_1 \simeq 0.4$ sec. Qualitatively, this can be understood by considering the hyperfine interaction as responsible for the relaxation. The tensor components perpendicular to the B_o direction are then responsible for the relaxation rate. Thus the 125 ppb component is only relaxed via the 15 ppb terms and has a long T_1 and vice versa. A quantitative discussion would be based on the knowledge of the tensor components at the individual carbon positions. These have become available from Reference 34, where high-resolution NMR techniques have been applied to unravel the individual couplings. Other work towards the same end have been published meanwhile.[42,43]

A different approach to spatial resolution of the conduction band spin density is by replacement of the protons in (FA) by deuterium. The ^2H magnetic moments

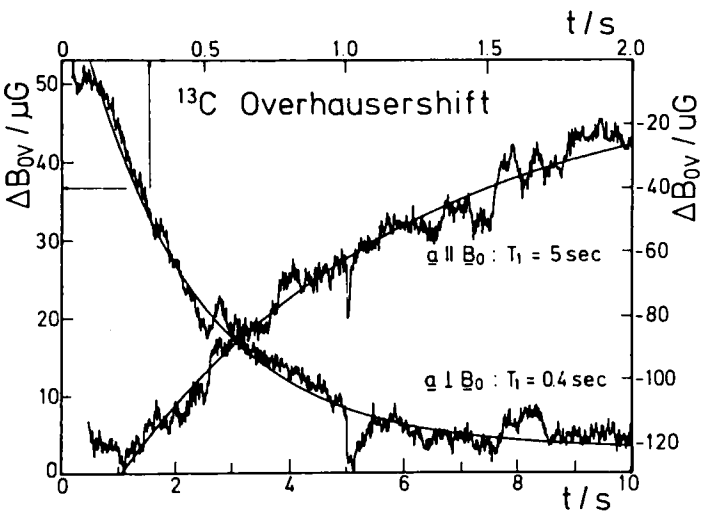

FIGURE 6 ^{13}C Overhauser shift versus time for two orientations of the magnetic field B_o. The larger negative $a \parallel B_o$ component displays a time constant $T_1 \simeq 5$ sec. The small positive $a \perp B_o$ component decays with ≈400 msec. The Larmor frequency is ≈3.6 MHz.

provide directional resolution via the quadrupole interaction. For I = 1 the NMR is split into two resonances separated by ΔE_Q. In the high B_o limit and for an axially symmetric quadrupole tensor, the splitting ΔE_Q amounts to

$$\Delta E_Q = \Delta Q \cdot (3 \cos^2\theta - 1) \tag{13}$$

where θ is the angle between the chemical bond axis and B_o and ΔQ is a constant characteristic for C—H bonds in hydrocarbons. Figure 7 shows the Overhauser shift of ^2H in $(FA)_2^+ PF_6^-$. For $B_o \parallel a$, all the individual bond angles are perpendicular to B_o, thus $\theta = 90°$ and the separation yields directly $\Delta Q = 140$ kHz. With B_o in the molecular plane, the different ^2H bonds lead to a separation on the frequency axis. Using Equation (13) and the orientation of the crystal with respect to B_o (known from the g-factor assignment), we are able to assign the different positions on the molecule. As is apparent from the lower two curves in Figure 7, only the nuclei at positions 3 and 8 show up significantly. The numbering is given in Figure 8. Due to the quadrupole splitting and the rather low γ of ^2H the individual lines are separated and there is no appreciable spin diffusion between different positions.

We have to extend Equation (11) (Overhauser shift) to the case of many magnetically inequivalent nuclei. The shift D^j of a nucleus at position j is given by:

$$D^j = 1/4 \cdot (\gamma_n/\gamma_e) \cdot A^j_{zz}/(kT) \cdot (1 + V^j \cdot S) \tag{14}$$

A^j is the hyperfine tensor of nucleus j and V^j is the enhancement factor, which can be different for different positions.

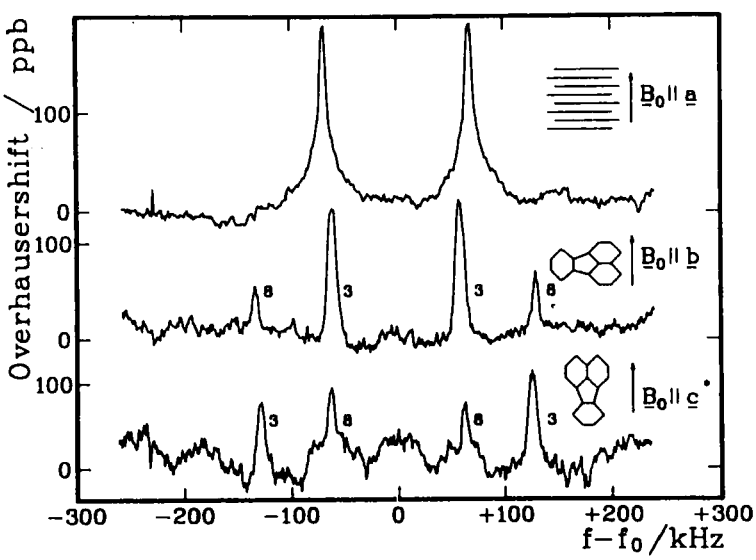

FIGURE 7 ^2H Overhauser shift with B_o along the three principal axes of the g-tensor: a) for $B_o \parallel a$, all ^2H contribute at the same resonance frequency. The observed quadrupole interaction is ≈140 kHz; b)–c) with $B_o \parallel b$ and $B_o \parallel c^*$, only position nos. 3 and 8 contribute significantly.

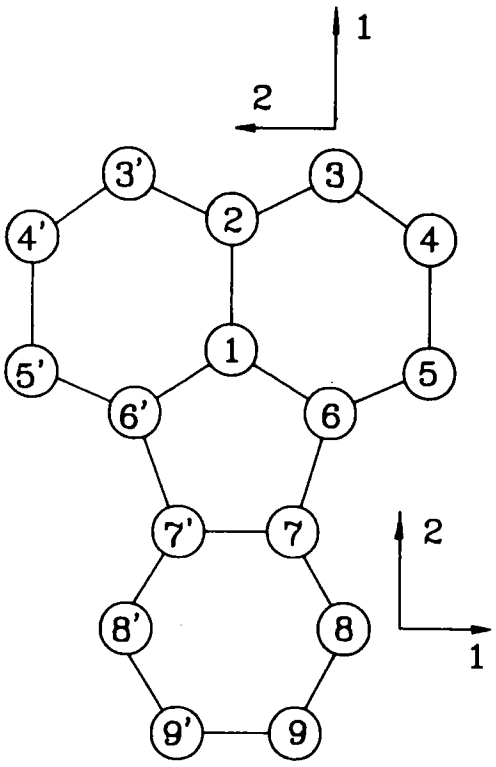

FIGURE 8 Orientation of the principal axes of the proton hyperfine tensors at molecular position 3 and 8. The third axis is perpendicular to the plane.

If the individual V^j were known, we could immediately calculate A^j. Since one expects the trace (A^j) to be proportional to the conduction electron spin density ρ at the corresponding carbon position, we could calculate ρ at the molecular positions 3, 4, 5, 8 and 9. This determination of the individual V^j has not yet been possible. However, we can conclude that:

1) The average enhancement factor $\langle V \rangle$ can be calculated from Equation (14) for the direction $B_o \parallel a$. From Figure 7 we have D = 185 ppb, which immediately yields $V_\parallel \simeq 1900$ for ^2H. The maximum possible enhancement would be $\gamma_e/\gamma_n = 4284$.

Thus the ratio V/V_{max} for ^1H and ^2H are nearly identical: $275/658 \simeq 0.42$ and $1990/4284 = 0.44$. This clearly shows, that the ^2H are predominantly relaxed via the electrons and that the quadrupole interaction is a negligible source of relaxation. This tells us, that the ^2H can be polarized to a high degree. In fact, we expect $V_\perp$ in the plane to be $\simeq 3600$, showing the high sensitivity of an Overhauser experiment.

2) The only significant spin density is in positions 3 and 8. However, we only detect the carbon positions connected to a proton (resp. ^2H). The spin density on positions 4, 5 and 9 is less than 30% the value at position 3 and 8.

3) The shift at position 8 is significantly less than the shift at position 3 for both orientations (Figure 7). Even without a detailed analysis we conclude, that the hyperfine tensor elements for position 8 must be smaller in value than the corresponding elements for tensor no. 3.

From a high resolution NMR experiment the proton hyperfine tensors at these two positions are now available (Reference 35). In this work two tensors were identified:

Tensor 1: A_{11}, A_{22}, A_{33} = (−3 MHz, −11 MHz, −6 MHz) and
Tensor 2: (−1 MHz, −9 MHz, −6 MHz).

Clearly we have to identify tensor 2 with the position 8 and tensor 1 with position 3. The Overhauser shift thus completes an assignment which could not be made by the Knight shift measurements alone.

CONCLUSION

Electron spin resonance allows detailed investigation of static and dynamic properties of the conduction electrons in radical cation salts. This is especially true, if double resonance techniques like the Overhauser shift method are employed. This method complements Knight shift measurements. Some of the techniques discussed in this contribution require the use of single crystals, others can be applied to polymers as well. Narrow ESR lines are an advantage, but we have demonstrated the applicability of the Overhauser shift technique for lines up to 200 μT in width. Technical improvements and higher ESR-frequency setups will extend the range to new materials.

Acknowledgments

It is a pleasure to acknowledge the contributions of W. Stöcklein, B. Gotschy (CW-ESR, pulsed ESR and Overhauser shift), R. Wagner, D. Schiller (diffusion measurements), G. Sachs (NMR, ESR) and J. Gmeiner crystal growth). I am particularly indebted to E. Dormann and M. Schwoerer for continuous support and stimulating suggestions and discussions. This work has been supported by Stiftung Volkswagenwerk and DFG (SFB 213).

References

1. T. C. Chiang, A. H. Reddoch and D. F. Williams, *J. Chem. Physics*, **54**, 2051 (1971).
2. H. P. Fritz, H. Gebauer, P. Friedrich, P. Ecker, R. Artes and U. Schubert, *Z. Naturforschung*, **83b**, 498 (1978).
3. Ch. Kröhnke, V. Enkelmann and G. Wegner, *Angewandte Chem.*, **92**, 941 (1980).
4. H. Eichele, M. Schwoerer, Ch. Kröhnke and G. Wegner, *Chem. Phys. Letters*, **77**, 311 (1981).
5. V. Enkelmann, *Chem. Phys.*, **66**, 303 (1982).
6. W. Stöcklein, B. Bail, M. Schwoerer, D. Singel and J. Schmidt, "Organic Molecular Aggregates" Proceedings of the Int. Symp. on Organic Materials at Schloss Elmau, eds. P. Reineker, H. Haken and H. C. Wolf, Springer Series in Solid-State Sciences, 49 (1983).
7. U. Köbler, J. Gmeiner and E. Dormann, *J. of Magnetism and Magnetic Materials*, **69**, 189 (1987).
8. W. Höptner, M. Mehring, J. U. von Schütz, H. C. Wolf, B. S. Morra, V. Enkelmann and G. Wegner, *Chem. Phys.*, **73**, 253 (1982).

9. W. Stöcklein and G. Denninger, *Mol. Cryst. Liq. Cryst.*, **136**, 335 (1986).
10. H. P. Geserich, B. Koch, W. Ruppel, R. Wilckens, D. Schweitzer, V. Enkelmann, G. Wegner, G. Wieners and H. J. Keller, *Journal de Physique*, **44**, 1461 (1983).
11. K. Bender, D. Schweitzer and H. J. Keller, *Journal de Physique*, **44**, C3-1433 (1983).
12. P. W. Anderson, *Rev. Mod. Phys.*, **25**, 269 (1959).
13. F. J. Dyson, *Phys. Rev.*, **98**, 349 (1954).
14. A. Kahn, *J. of Applied Phys.*, **46**, 4965 (1975).
15. A. J. Stone, *Mol. Phys.*, **6**, 509 (1963).
16. K. Möbius, *Z. Naturforschung*, **20a**, 1093 (1965).
17. B. G. Segal, *Chem. Phys.*, **43**, 4191 (1965).
18. R. Angstl, *Chem. Phys.*, submitted (1988).
19. R. J. Elliot, *Phys. Rev.*, **96**, 266 (1954).
20. F. Beuneu and P. Monod, *Phys. Rev.*, **B18**, 2422 (1978).
21. Y. Tomkiewicz and A. R. Taranko, *Phys. Rev.*, **B18**, 733 (1978).
22. G. Sachs, W. Stöcklein, B. Bail, E. Dormann and M. Schwoerer, *Chem. Phys. Letts.*, **89**, 179 (1982).
23. J. Sigg, Th. Prisner, K. P. Dinse, H. Brunner, D. Schweitzer and K. H. Hausser: a) *Journal de Physique*, **44**, C3-1421 (1983); b) *Phys. Rev.*, **B27**, 5366 (1983).
24. W. Stöcklein, Dissertation, Universität Bayreuth (1985).
25. H. C. Torrey, *Phys. Rev.*, **104**, 563 (1956).
26. G. G. Maresch, M. Mehring, J. U. von Schütz and H. C. Wolf, *Chem. Phys.*, **85**, 333 (1984).
27. G. G. Maresch, A. Grupp, M. Mehring, J. U. von Schütz and H. C. Wolf, *Journal de Physique*, **46**, 461 (1985).
28. G. Sachs and E. Dormann, submitted to *Synth. Metals* (1988).
29. J. Korringa, *Physica*, **16**, 601 (1950).
30. A. W. Overhauser: a) *Phys. Rev.*, **89**, 689 (1953); b) *Phys. Rev.*, **92**, 411 (1953).
31. G. Feher, *Phys. Rev.*, **105**, 1122 (1957).
32. Ch. Ryter, *Phys. Rev.*, **5**, 10 (1960).
33. W. G. Clark, J. Hamman, J. Sanny and L. C. Tippie, "*Quasi One-Dimensional Conductors II*," Proceedings, Dubrovnik, 1978.
34. M. Mehring and J. Spengler, *Phys. Rev. Lett.*, **53**, 2441 (1984).
35. F. Hentsch, M. Helmle, D. Köngeter and M. Mehring, *Phys. Rev.*, **B37**, 7205 (1988).
36. D. Köngeter and M. Mehring, *Phys. Rev. B*, submitted (1988).
37. G. Denninger, W. Stöcklein, E. Dormann and M. Schwoerer, *Chem. Phys. Lett.*, **107**, 222 (1984).
38. G. Denninger, E. Dormann and M. Schwoerer, *Synthetic Metals*, **19**, 355 (1987).
39. B. Gotschy and G. Denninger, to be published.
40. I. Solomon, *Phys. Rev.*, **99**, 559 (1955).
41. H. Brunner, K. H. Hausser, H. J. Keller and D. Schweitzer, *Solid State Comm.*, **51**, 107 (1984).
42. W. Stöcklein, H. Seidel, D. Singel, R. D. Kendrick and C. S. Yannoni, *Chem. Phys. Lett.*, **141**, 277 (1987).
43. R. A. Wind, H. Lock and M. Mehring, *Chem. Phys. Lett.*, **141**, 283 (1987).
44. M. Schwoerer, "Proceedings XXIII Congress Ampere," Roma, 81, eds. B. Maraviglia, F. De Luca and R. Campanella (1986).